

A Homotopy-based Algorithm for Sparse Multiple Right-hand Sides Nonnegative Least Squares

Nicolas Nadisic¹ · Arnaud Vandaele¹ ·
Nicolas Gillis¹

Received: date / Accepted: date

Abstract Nonnegative least squares (NNLS) problems arise in models that rely on additive linear combinations. In particular, they are at the core of nonnegative matrix factorization (NMF) algorithms. The nonnegativity constraint is known to naturally favor sparsity, that is, solutions with few non-zero entries. However, it is often useful to further enhance this sparsity, as it improves the interpretability of the results and helps reducing noise. While the ℓ_0 -“norm”, equal to the number of non-zeros entries in a vector, is a natural sparsity measure, its combinatorial nature makes it difficult to use in practical optimization schemes. Most existing approaches thus rely either on its convex surrogate, the ℓ_1 -norm, or on heuristics such as greedy algorithms. In the case of multiple right-hand sides NNLS (MNNLS), which are used within NMF algorithms, sparsity is often enforced column- or row-wise, and the fact that the solution is a matrix is not exploited. In this paper, we first introduce a novel formulation for sparse MNNLS, with a matrix-wise ℓ_0 sparsity constraint. Then, we present a two-step algorithm to tackle this problem. The first step uses a homotopy algorithm to produce the whole regularization path for all the ℓ_1 -penalized NNLS problems arising in MNNLS, that is, to produce a set of solutions representing different tradeoffs between reconstruction error and sparsity. The second step selects solutions among these paths in order to build a sparsity-constrained matrix that minimizes the reconstruction error. We illustrate the advantages of our proposed algorithm for the unmixing of facial and hyperspectral images.

Keywords nonnegative least squares · sparsity · nonnegative matrix factorization · homotopy algorithm

NN and NG acknowledge the support by the European Research Council (ERC starting grant No 679515), and by the Fonds de la Recherche Scientifique - FNRS and the Fonds Wetenschappelijk Onderzoek - Vlanderen (FWO) under EOS project O005318F-RG47.

✉ Nicolas Nadisic
nicolas.nadisic@umons.ac.be

¹ Department of Mathematics and Operational Research, University of Mons, Mons, Belgium

1 Introduction

Nonnegative least squares (NNLS) problems arise in many applications where data points can be represented as additive linear combinations of meaningful components (Lee and Seung, 1997). For instance,

- In facial images, the faces are the nonnegative linear combination of facial features such as eyes, noses and lips (Lee and Seung, 1999).
- In hyperspectral images, the spectral signature of a pixel is the nonnegative linear combination of the spectral signature of the materials it contains (Bioucas-Dias et al, 2012).

NNLS problems are also at the core of many alternating approaches to solve non-negative matrix factorization (NMF) (Gillis, 2014b). The standard NNLS problem using least squares can be formulated as follows

$$\min_{x \in \mathbb{R}^r} \frac{1}{2} \|Ax - b\|_2^2 \quad \text{such that} \quad x \geq 0, \quad (1)$$

where $A \in \mathbb{R}^{m \times r}$, and $b \in \mathbb{R}^m$.

1.1 Sparsity and NNLS

The nonnegativity constraint is known to naturally produce sparse solutions, that is, solutions with few non-zero entries (Foucart and Koslicki, 2014). Sparsity often improves the interpretability of the results by modelling data points as combinations of only a few components. For example, in hyperspectral unmixing, that is, the task of identifying materials in a hyperspectral image, sparsity means that a pixel contains only a few materials. Unfortunately, the sparsity of the solution to a NNLS problem is not guaranteed in general, whereas controlling it can be helpful in many applications. For this reason, numerous techniques have been developed to favor sparsity.

A natural sparsity measure is the ℓ_0 -“norm”, defined as the number of non-zero entries in a given vector, $\|x\|_0 = |\{i : x_i \neq 0\}|$. Given a positive integer k , a vector x is k -sparse if $\|x\|_0 \leq k$. A sparsity-constrained variant of Problem (1), referred to as k -sparse NNLS, is the following

$$\min_{x \in \mathbb{R}^r} \frac{1}{2} \|Ax - b\|_2^2 \quad \text{such that} \quad x \geq 0 \quad \text{and} \quad \|x\|_0 \leq k. \quad (2)$$

Albeit intuitive and easily interpretable, the constraint of k -sparsity is hard to enforce in practice, because the ℓ_0 -“norm” is non-convex and non-smooth.

For this reason, practitioners often prefer other sparsity-inducing approaches, such as ℓ_1 -regularization. The ℓ_1 -norm, defined as $\|x\|_1 = \sum_{i=1}^r |x_i|$, is a convex surrogate of the ℓ_0 -“norm”, it is therefore easier to optimize in practice while being a good sparsity measure. The ℓ_1 -regularization consists in penalizing the solution in the objective function of (1), leading to the following problem, referred to as ℓ_1 -NNLS,

$$\min_{x \in \mathbb{R}^r} \frac{1}{2} \|Ax - b\|_2^2 + \lambda \|x\|_1 \quad \text{such that} \quad x \geq 0. \quad (3)$$

Note that, without the nonnegativity constraint, this is the well-known LASSO model (Tibshirani, 1996). Problem (3) can be thought of as the weighted-sum form of a multiobjective problem, where the objectives are minimizing the reconstruction error $\frac{1}{2}\|Ax - b\|_2^2$ on one hand, and minimizing the ℓ_1 -norm of the solution $\|x\|_1$ on the other hand. The former measures the quality of the solution, while the latter favors its sparsity. The parameter λ controls the trade-off between the two objectives.

Despite its popularity, this technique suffers from several drawbacks. In particular, there is no explicit relation between the parameter λ and the sparsity of the solution, hence choosing an appropriate value for λ can be tricky, and often involves a tedious trial-and-error process. Also, the ℓ_1 -penalty introduces a bias. Although there exist theoretical guarantees for support recovery, such as the *Exact Recovery Condition* (Tropp, 2006), they are restrictive and often not realistic in practice.

To overcome these issues, *homotopy* methods have been introduced that generate the full *regularization path* of a given ℓ_1 -NNLS problem, that is, the set of the solutions for all possible values of λ . They allow the user to choose the relevant solution within this path, each solution representing a different trade-off between sparsity and reconstruction error. The first homotopy method has been introduced by Osborne et al (2000), for sparse least squares with no nonnegativity constraint. Variants have been developed by Efron et al (2004) and Donoho and Tsai (2008). Kim et al (2013) introduced a variant to deal specifically with the nonnegativity constraint. We detail the homotopy method for NNLS in Section 3.

1.2 Sparsity and multiple right-hand sides NNLS

In many applications, we have to deal with multiple right-hand sides NNLS problems (MNNLS), that is, problems of the form

$$\min_H \frac{1}{2} \|M - WH\|_2^2 \quad \text{such that} \quad H \geq 0, \quad (4)$$

where $M \in \mathbb{R}^{m \times n}$, $W \in \mathbb{R}^{m \times r}$, and $H \in \mathbb{R}^{r \times n}$. We note $M(:, j)$ the j -th column of the matrix M . Problem (4) can be decomposed into n NNLS subproblems of the form (1), where $H(:, j)$, W , and $M(:, j)$ correspond to x , A , and b , respectively. For example, in the unmixing of a hyperspectral image, every column $M(:, j)$ represents a pixel, and the corresponding column $H(:, j)$ represents its composition, in terms of the abundances of the r materials whose spectral signatures are the columns of W . In this work, for the sake of conciseness, we focus only on the (sparse) optimization of H , but all concepts and algorithms can be applied symmetrically on W .

This is related to the nonnegative matrix factorization (NMF) problem, of the form

$$\min_{W, H} \frac{1}{2} \|M - WH\|_F^2 \quad \text{such that} \quad W \geq 0 \text{ and } H \geq 0, \quad (5)$$

in which we aim at finding the factors W and H , given M and a factorization rank r . The usual optimization scheme for NMF consists in alternatively optimizing one factor while fixing the other, which is equivalent to solving MNNLS subproblems.

To encourage sparsity in MNNLS, one can apply a sparse NNLS model column-wise, leading to

$$\min_H \frac{1}{2} \|M - WH\|_2^2 \quad \text{such that} \quad H \geq 0 \text{ and } \|H(:,j)\|_0 \leq k \text{ for all } j. \quad (6)$$

However, in some applications, setting the sparsity parameter k is tricky, as the relevant value can vary for different columns. For example, in hyperspectral unmixing, pixels will be composed of different numbers of materials. Therefore, one can consider a more global approach, such as

$$\min_H \frac{1}{2} \|M - WH\|_2^2 \quad \text{such that} \quad H \geq 0 \text{ and } \|H\|_0 \leq q, \quad (7)$$

where $\|H\|_0 = \sum_j \|H(:,j)\|_0$ and q is a matrix-wise sparsity parameter, hence enforcing an *average* sparsity q/n for the columns of H .

1.3 Contribution and outline of the paper

In this work, we present an approximate method to solve Problem (7). Our approach consists in using a homotopy method to compute a regularization path for every column of H , and then exploit these paths with a dedicated optimization algorithm to build a solution to Problem (7).

The paper is organized as follows. In Section 2, we present existing approaches for sparse NNLS and sparse MNNLS. In Section 3, we detail the homotopy principle and algorithm. In Section 4, we present the main contribution of this work, that is, an algorithm to solve Problem (7). We illustrate the effectiveness of our proposed algorithm with experiments on real-life facial and hyperspectral image datasets in Section 5, and conclude in Section 6.

2 Related work

We discussed in Section 1.1 the methods based on the ℓ_1 -norm, and their limitations. In this section, we first discuss the existing works that solve the ℓ_0 -constrained problem, as defined in Problem (2). We then review the most common approaches for sparse MNNLS.

2.1 k -sparse NNLS

Greedy algorithms are one of the most popular approaches for solving Problem (2). They start with an empty support ($x_i = 0$ for all i), and select components one by one to enrich the support, until the target sparsity k is reached. The selection of a component is done greedily, by choosing the component maximizing the decrease of the residual error. Orthogonal versions of these methods, such as *Orthogonal Least Squares* (OLS) (Chen et al, 1989) and *Orthogonal Matching Pursuit* (OMP) (Pati et al, 1993) make sure a component can be selected only once. Nonnegative variants have been proposed recently; see for example Nguyen et al (2019) and the references therein. In general, these algorithms do not give the

globally optimal solution. Again, theoretical recovery guarantees exist, but they are restrictive (Soussen et al, 2013).

Other works were proposed for solving globally the ℓ_0 -constrained problem, although not specifically with nonnegativity constraints. Notably, Bienstock (1996) proposed a reformulation of Problem (2) to a mixed-integer program (MIP), and a branch-and-cut algorithm to solve it, using continuous relaxation at every iteration. Several contributions extended this approach, for example under different constraints, or using new methods to solve the continuous relaxation subproblem; see for example Bertsimas and Shioda (2009); Bourguignon et al (2015) and the references therein. Mhenni et al (2019) further extended it, using a homotopy algorithm to compute the relaxations.

2.2 Sparse MNNLS

Most approaches that tackle sparse MNNLS were actually introduced in the context of sparse NMF. Since its very introduction by Lee and Seung (1999), NMF is appreciated for the sparsity of the produced factors. A variety of works have been proposed to further enhance this sparsity, making *sparse NMF* one of the most popular variants of NMF. Many authors worked on the ℓ_1 -penalized formulation, notably Hoyer (2002); Eggert and Korner (2004); Kim and Park (2007); Cichocki et al (2008); Gillis (2012).

To avoid the issues linked to the ℓ_1 -penalty, Hoyer (2004) introduced a more explicit sparsity measure, based on the ratio between the ℓ_1 -norm and the ℓ_2 -norm, and considered an NMF variant with a column-wise constraint on this measure. Other works considered the ℓ_0 -“norm” formulation, that can be decomposed into a series of k -sparse NNLS subproblems. We can cite Aharon et al (2005); Morup et al (2008); Peharz and Pernkopf (2012). Cohen and Gillis (2019) proposed a method that solves *exactly* the k -sparse NNLS subproblems, using a brute-force approach. Nadisic et al (2020) extended this work by replacing the brute-force subroutine by a dedicated branch-and-bound algorithm.

3 The homotopy algorithm

In this section, we review the homotopy method, which is central in our proposed algorithm for solving Problem (7).

Given an ℓ_1 -NNLS problem, the homotopy algorithm computes sequentially all optimal solutions for the different values of λ . In a nutshell, it uses the KKT conditions (necessary conditions for optimality) to first find the value λ_{\max} for which the optimal solution of ℓ_1 -NNLS is $x = 0$ for any $\lambda \geq \lambda_{\max}$, and then to compute the next smaller values of λ for which the support (that is, the set of non-zero entries) of the optimal solution changes (one zero entry becomes non-zero, or the other way around). This is similar in spirit to active-set methods, akin to the simplex algorithm for linear programming. These values of λ are called *breakpoints*, between which the support of the optimal solution does not change. We denote the first breakpoint λ_{\max} , and the following ones $\lambda_2, \lambda_3, \dots$; see Figs. 1 and 2 for an illustration.

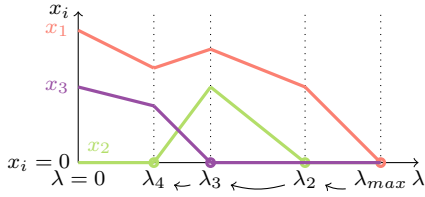


Fig. 1 Example of a solution path of a homotopy algorithm, depending on λ , for a problem of 3 variables. Vertical dotted lines correspond to breakpoints.

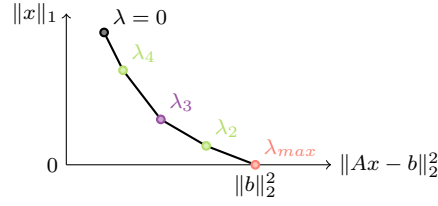


Fig. 2 Trade-off between the ℓ_1 -norm and the error $\|Ax - b\|_2^2$ corresponding to the solution path in Fig. 1.

3.1 Optimality conditions

The homotopy algorithm uses the first-order optimality conditions, that is, the KKT conditions, to determine the breakpoints and the supports of the corresponding solutions. Because x is nonnegative, we have $\|x\|_1 = \sum_i x_i = e^T x$, where e is the vector of all ones whose dimension will be clear from context. Therefore, the ℓ_1 -NNLS problem can be written as follows

$$\min_{x \geq 0} f(x), \text{ where } f(x) = \frac{1}{2} \|Ax - b\|_2^2 + \lambda e^T x. \quad (8)$$

The KKT conditions are $x \geq 0$,

$$\nabla f(x) = \underbrace{A^T A x}_P - \underbrace{A^T b}_\ell + \lambda e \geq 0, \quad (9)$$

$$x_i (A^T A x - A^T b + \lambda e)_i = 0 \text{ for all } i. \quad (10)$$

Eq. (10) is the complementary condition; for every entry of x , either the entry itself or the corresponding gradient entry is equal to zero. To simplify the notation, let us define $P = A^T A$ and $\ell = A^T b$.

As f is a convex function and the feasible set contains a Slater point (e.g., $x = e$), the KKT conditions are necessary and sufficient. Therefore, any solution x satisfying them is optimal. Suppose we know the optimal support, that is, the set \mathcal{K} such that $x(\mathcal{K}) > 0$ and $x(\bar{\mathcal{K}}) = 0$, where $\bar{\mathcal{K}} = \{1, 2, \dots, n\} \setminus \mathcal{K}$. Then

$$\begin{aligned} x(\mathcal{K}) > 0 &\Rightarrow P(\mathcal{K}, \mathcal{K})x(\mathcal{K}) - \ell(\mathcal{K}) + \lambda e = 0 \\ &\Rightarrow x(\mathcal{K}) = P(\mathcal{K}, \mathcal{K})^{-1}(\ell(\mathcal{K}) - \lambda e) \geq 0, \end{aligned} \quad (\mathcal{C1})$$

and

$$Px - \ell + \lambda e \geq 0 \Rightarrow P(\bar{\mathcal{K}}, \mathcal{K})x(\mathcal{K}) - \ell(\bar{\mathcal{K}}) + \lambda e \geq 0. \quad (\mathcal{C2})$$

Replacing $x(\mathcal{K})$ in (C2) by (C1), we have

$$P(\bar{\mathcal{K}}, \mathcal{K})[P(\mathcal{K}, \mathcal{K})^{-1}(\ell(\mathcal{K}) - \lambda e)] - \ell(\bar{\mathcal{K}}) + \lambda e \geq 0.$$

Let us simplify the notation. Let

$$a_{\mathcal{K}} = P(\mathcal{K}, \mathcal{K})^{-1}\ell(\mathcal{K}), \text{ and } b_{\mathcal{K}} = P(\mathcal{K}, \mathcal{K})^{-1}e. \quad (11)$$

We can rewrite (C1) as

$$a_{\mathcal{K}} - \lambda b_{\mathcal{K}} \geq 0. \quad (\text{C1b})$$

Note that the dimension of $a_{\mathcal{K}}$ and $b_{\mathcal{K}}$ is the cardinality of \mathcal{K} . Let

$$c_{\mathcal{K}} = P(\bar{\mathcal{K}}, \mathcal{K})a_{\mathcal{K}} - \ell(\bar{\mathcal{K}}), \text{ and } d_{\mathcal{K}} = P(\bar{\mathcal{K}}, \mathcal{K})b_{\mathcal{K}} - e.$$

We can rewrite (C2) as

$$c_{\mathcal{K}} - \lambda d_{\mathcal{K}} \geq 0. \quad (\text{C2b})$$

Note that the dimension of $c_{\mathcal{K}}$ and $d_{\mathcal{K}}$ is the cardinality of $\bar{\mathcal{K}}$. Moreover, Equations (C1b) and (C2b) are linear in λ : Given \mathcal{K} , we can easily compute $a_{\mathcal{K}}$, $b_{\mathcal{K}}$, $c_{\mathcal{K}}$, $d_{\mathcal{K}}$.

3.2 Algorithm description

The goal of the homotopy algorithm is to compute breakpoints and their corresponding supports. It starts with an empty support, corresponding to the zero vector for any $\lambda \geq \lambda_{max}$, and iteratively adds or removes entries to the support while decreasing the value of λ .

The first step to build the regularization path is to find the first breakpoint λ_{max} , that is, the minimum value of λ such that the solution is the zero vector. If the optimal solution is $x = 0$, that is, $\mathcal{K} = \emptyset$ and $\bar{\mathcal{K}} = \{1, 2, \dots, n\}$, then from Eq. (9) we have $\lambda \geq \max_i \ell_i$. Therefore, the first breakpoint is

$$\lambda_{max} = \max_i \ell_i = \max_i (A^T b)_i = \max_i A(:, i)^T b.$$

The index $i_1 = \arg \max_i \ell_i$ is the first to enter the support¹, thus for $\lambda_2 \leq \lambda < \lambda_{max}$ we have $\mathcal{K} = \{i_1\}$.

From a given support \mathcal{K}_j , the next breakpoint $\lambda_{j+1} \leq \lambda_j$ is the largest value of λ that violates one of the conditions (C1) or (C2). If (C1) is violated then a variable will leave the support, that is, a positive entry will become zero. Denoting k^* the index of this entry, we have $\mathcal{K}_{j+1} = \mathcal{K}_j \setminus \{k^*\}$. If (C2) is violated then a variable will enter the support, that is, a zero entry will become positive, $\mathcal{K}_{j+1} = \mathcal{K}_j \cup \{k^*\}$.

Let us consider (C1). We have $a_{\mathcal{K}}(k) - \lambda b_{\mathcal{K}}(k) \geq 0$ for all k so

$$\lambda_{j+1} \geq \max_{\{k | b_{\mathcal{K}}(k) < 0\}} \frac{a_{\mathcal{K}}(k)}{b_{\mathcal{K}}(k)}.$$

Similarly, for (C2) we have $c_{\mathcal{K}}(k) - \lambda d_{\mathcal{K}}(k) \geq 0$ for all k so

$$\lambda_{j+1} \geq \max_{\{k | d_{\mathcal{K}}(k) < 0\}} \frac{c_{\mathcal{K}}(k)}{d_{\mathcal{K}}(k)}.$$

Therefore,

$$\lambda_{j+1} = \max \left(\underbrace{\max_{\{k | b_{\mathcal{K}}(k) < 0\}} \frac{a_{\mathcal{K}}(k)}{b_{\mathcal{K}}(k)}}_{\text{Case 1}}, \underbrace{\max_{\{k | d_{\mathcal{K}}(k) < 0\}} \frac{c_{\mathcal{K}}(k)}{d_{\mathcal{K}}(k)}}_{\text{Case 2}} \right).$$

¹ If two or more columns maximize the value of ℓ_i , we have to pick one to start the homotopy. If we always pick the one with smallest index, then the algorithm behaves normally, except that at the next iteration we will have $\lambda_{j+1} = \lambda_j$. This is similar to Bland's rule for the simplex algorithm.

The algorithm is detailed formally in Algorithm 1. Note that, inside the algorithm loop, once a support \mathcal{K} is identified, getting the corresponding optimal solution is straightforward. From Eq. (11), if $a_{\mathcal{K}}$ is nonnegative, then the unbiased optimal solution of the NNLS problem is the vector x^* such that $x^*(\bar{\mathcal{K}}) = 0$ and $x^*(\mathcal{K}) = a_{\mathcal{K}}$. If $a_{\mathcal{K}}$ has negative entries, then we can compute the unbiased solution with a standard NNLS solver, with $x^*(\bar{\mathcal{K}}) = 0$ and $x^*(\mathcal{K}) = \arg \min_{x \geq 0} \|P(\mathcal{K}, \mathcal{K})x - l(\mathcal{K})\|_2^2$.

Algorithm 1: Homotopy algorithm for sparse NNLS

Input: $A \in \mathbb{R}^{m \times r}$, $b \in \mathbb{R}^m$
Output: Breakpoints λ_j , corresponding supports \mathcal{K}_j and solutions x_j^* , for all j

- 1 $i_1 \leftarrow \arg \max_i \ell_i$
- 2 $K \leftarrow \{i_1\}$; $\lambda_1 = \lambda_{\max} = \ell_{i_1}$, $j \leftarrow 1$
- 3 **while** $\lambda_j > 0$ **do**
- 4 $j \leftarrow j + 1$
- 5 Compute a_K, b_K, c_K, d_K
- 6 $\lambda_{C1} \leftarrow \max_{\{k | b_{\mathcal{K}}(k) < 0\}} \frac{a_{\mathcal{K}}(k)}{b_{\mathcal{K}}(k)}$, and $k_{C1}^* \leftarrow$ corresponding argmax
- 7 $\lambda_{C2} \leftarrow \max_{\{k | d_{\mathcal{K}}(k) < 0\}} \frac{c_{\mathcal{K}}(k)}{d_{\mathcal{K}}(k)}$, and $k_{C2}^* \leftarrow$ corresponding argmax
- 8 **if** $\lambda_{C1} \geq \lambda_{C2}$ **then**
- 9 $\lambda_j \leftarrow \lambda_{C1}$
- 10 $\mathcal{K} \leftarrow \mathcal{K} \setminus \{k_{C1}^*\}$
- 11 **else if** $\lambda_{C1} < \lambda_{C2}$ **then**
- 12 $\lambda_j \leftarrow \lambda_{C2}$
- 13 $\mathcal{K} \leftarrow \mathcal{K} \cup \{k_{C2}^*\}$
- 14 $x_j^*(\bar{\mathcal{K}}) \leftarrow 0$
- 15 **if** $a_{\mathcal{K}} > 0$ **then**
- 16 $x_j^*(\mathcal{K}) \leftarrow a_{\mathcal{K}}$
- 17 **else**
- 18 $x_{\mathcal{K}}^* = \arg \min_{x \geq 0} \|P(\mathcal{K}, \mathcal{K})x - \ell(\mathcal{K})\|_2^2$

3.3 Computational cost

As explained by Kim et al (2013), the time complexity of one iteration of the homotopy algorithm is the same as one iteration of the standard active-set algorithm (Lawson and Hanson, 1995), that is, $\mathcal{O}(r^3)$ operations. It is dominated by the computation of $a_{\mathcal{K}}$, that entails solving a linear system in at most r variables. The number of iterations equals the number of breakpoints, which is in practice similar to those of the active-set. In the worst case, active-set methods might require an exponential number of iterations, up to $\mathcal{O}(2^r)$, as the simplex algorithm for linear programming. However, in practice, we have observed that it typically requires much less iterations, of the order of $\mathcal{O}(r)$. In particular, when P^{-1} is diagonally dominant, we have $b_{\mathcal{K}} > 0$, so (C1) is never violated. As a result, when λ decreases, no positive entry of x becomes zero. We only add entries to the support, so the homotopy algorithm will be done in at most r iterations. In practice, even when

this condition is not met, we have observed that adding entries to the support happens far more often than removing entries.

As the homotopy algorithm solves a series of ℓ_1 -penalized NNLS problems, there exist conditions under which it is guaranteed to recover the correct supports, that is, the supports of the solutions of the corresponding ℓ_0 -constrained NNLS problems; see Itoh et al (2017) and the references therein.

4 Proposed algorithm for sparse MNNLS

In this section, we present the main contribution of our work, that is, how we leverage the NNLS homotopy algorithm to solve Problem (7). First of all, given the data matrix M and the dictionary W , we run the homotopy algorithm for every column of M , that is, with input $A = W$ and $b = M(:, j)$ for all j . This gives us the set of supports of the optimal solutions of the ℓ_1 -regularized NNLS for every column of M , for all values of λ . From these sets, we build a cost matrix \mathcal{C} where each column represents a column j of H , each row represents a k -sparsity between 0 and r , and each entry is the error $\|M(:, j) - WH(:, j)\|_2^2$ of the k -sparse solution of column j . When this is done, we need to select one solution per column to build the solution matrix H , that is, we need to choose the sparsity level for each column of H . This selection is a combinatorial problem, similar to an assignment problem. It can be tackled in many different ways. For instance, one can trivially select the k -sparse solution for every column, thus reducing to Problem (6). In the following, we propose a global selection strategy that solves the selection subproblem exactly.

We call our algorithm² SHAMANS, and detail it in Algorithm 2. Note that we do not use the values of the breakpoints λ ; we only use the regularization path, that is, the solutions x^* and their supports \mathcal{K} . Let us explain how SHAMANS proceeds.

First, between lines 1 and 11, the homotopy algorithm is used to compute k -sparse solutions for the columns of H , as explained above. On line 3, we begin to loop over the columns of M . On line 4, we call the homotopy algorithm and store the resulting solutions and their supports. Between line 5 and line 11, we build the cost matrix \mathcal{C} such that every column $\mathcal{C}(:, j)$ corresponds to the subproblem $\min_{x \geq 0} \|M(:, j) - Wx\|_2^2$, that is, to the computation of the column $H(:, j)$, and every row corresponds to a value of k , between 0 and r . An entry of \mathcal{C} thus represents the reconstruction error of the k -sparse solution for the column $H(:, j)$ obtained with the homotopy. The corresponding $Sol_{k,j}$ stores this solution. The loop on line 9 allows, when updating a k -sparse solution, to also update the k' -sparse solutions, with k' greater than k . This is necessary so that, if a k -sparse solution has a lower reconstruction error than a k' -sparse solution with $k' > k$ (although this case is unlikely to happen), then the entry corresponding to k' will contain the k -sparse solution. It is also useful when, for a given column and for some k , a k -sparse solution does not exist because the homotopy algorithm does not necessarily generate k -sparse solutions for all $k = 0, 1, 2, \dots, r$. Note that, with $k < k'$, a k -sparse vector x_k is also k' -sparse, because $\|x_k\|_0 \leq k < k'$.

The selection step, between lines 12 and 27, begins with the initialization of the cursors. There is one cursor Cur_j for every column $H(:, j)$, and it indicates

² The name stands for “SHAMANS is a Homotopy-based Algorithm for Matrix Approximation under Nonnegativity and Sparsity”

Algorithm 2: SHAMANS

Input: Data matrix $M \in \mathbb{R}^{m \times n}$, dictionary $W \in \mathbb{R}^{m \times r}$, sparsity target $q \in \mathbb{N}$
Output: $H^* \in \mathbb{R}^{r \times n}$, $H^* = \arg \min_{H \geq 0} \|M - WH\|_F^2$ s.t. $\|H\|_0 \leq q + r - 1$

- 1 Init matrix $C \in \mathbb{R}^{r \times n}$, $\forall i, \forall j, C(i, j) \leftarrow \infty$
- 2 Init solutions $Sol_{i,j}$
- 3 **foreach** $j \in \{1, \dots, n\}$ **do**
- 4 $\{K_t, x_t^*\}_{\forall t} \leftarrow \text{homotopy}(W, M(:, j))$
- 5 **foreach** t **do**
- 6 $k \leftarrow |K_t|$
- 7 $err \leftarrow \|M(:, j) - Wx_t^*\|_2^2$
- 8 **if** $err < C(k, j)$ **then**
- 9 **foreach** $i \in \{k, \dots, r\}$ **do**
- 10 $C(i, j) \leftarrow err$
- 11 $Sol_{i,j} \leftarrow x_t^*$
- 12 Init cursors, $\forall j, Cur_j \leftarrow 0$
- 13 Init matrix $\Delta C \in \mathbb{R}^{r \times n}$
- 14 Init matrix $\mathcal{G} \in \mathbb{R}^{r \times n}$
- 15 **foreach** $i \in \{1, \dots, r\}, j \in \{1, \dots, n\}$ **do**
- 16 $\Delta C(i, j) \leftarrow C(i-1, j) - C(i, j)$
- 17 **foreach** $i \in \{1, \dots, r\}, j \in \{1, \dots, n\}$ **do**
- 18 $\mathcal{G}(i, j) \leftarrow (\sum_{l=1}^i \Delta C(l, j)) / i$
- 19 $it \leftarrow 0$
- 20 **while** $it < q$ **do**
- 21 $i^*, j^* \leftarrow \arg \max \mathcal{G}$
- 22 $it \leftarrow i^* - Cur_{j^*}$
- 23 $Cur_{j^*} = i^*$
- 24 **foreach** $i \in \{i^* + 1, \dots, r\}$ **do**
- 25 $\mathcal{G}(i, j^*) \leftarrow \frac{\sum_{l=i^*+1}^i \Delta C(l, j^*)}{(i-i^*)}$
- 26 **foreach** $j \in \{1, \dots, n\}$ **do**
- 27 $H^*(:, j) = Sol_{Cur_j, j}$

the number of non-zero entries selected in the current solution (that is, the k -sparsity of the currently selected solution) for this column. We begin with all cursors at zero, meaning that the 0-sparse solution (the zero vector) is selected for each column. We then increment one cursor at every iteration by selecting new non-zero entries until the sparsity target is reached. We first compute the matrix ΔC (lines 15 and 16). An entry $\Delta C(k, j)$ represents, for the column $H(:, j)$, the error decrease when going from the $(k-1)$ -sparse solution to the k -sparse one. An example of such a matrix is given in Section 4.1. From ΔC , we then build a matrix \mathcal{G} (lines 17 and 18), that is essentially ΔC with entries divided by the corresponding k . Every entry of \mathcal{G} then represents the error decrease of a solution, divided by the corresponding cost in sparsity budget. Finally, at every iteration, SHAMANS selects the maximum entry in \mathcal{G} (line 21), guaranteeing to have the largest possible decrease of the error $\|M - WH\|_F^2$ for a fixed budget of additional non-zero entries in H (at each step, there will be between 1 and r new non-zero entries in H). Note that this operation is very cheap in practice, as we can implement it by maintaining a sorted list of the maximum entry of each column, and thus avoid to recompute the maximum over the whole matrix. We use its coordinates

to update the cursor (line 23). After every iteration, the column of \mathcal{G} of the last selected solution must be updated (lines 24 and 25). If the last selected solution is k -sparse, then all the entries corresponding to k' -sparse solutions with $k' < k$ are put to zero in the corresponding column of \mathcal{G} , so they will not be selected during the next iterations. The entries corresponding to k' -sparse solutions with $k' > k$ are recomputed from $\Delta\mathcal{C}$ to take into account the new value of the cursor. In other words, the corresponding column of \mathcal{G} maintains the reduction in the error $\|M(:,j) - WH(:,j)\|_2^2$ if we further add non-zero entries in $H(:,j)$. Finally, on lines 26 and 27, we build the matrix H^* with the final cursors. In Section 4.1, we illustrate SHAMANS with a toy example.

Finally, although motivated by nonnegative problems, our approach is generalized easily to problems with no nonnegativity constraint. In SHAMANS, the selection step is not specific to nonnegativity, and the homotopy step for sparse NNLS can be easily replaced with a standard homotopy algorithm for sparse LS.

4.1 Running example for SHAMANS

Let us consider the following example, with the 5-by-6 data matrix M and the 5-by-4 dictionary W :

$$M = \begin{pmatrix} 0.89 & 1.21 & 0.73 & 0.8 & 0.06 & 0.02 \\ 0.65 & 0.97 & 1.17 & 0.23 & 0.36 & 0.27 \\ 1.06 & 1.63 & 1.27 & 0.76 & 0.49 & 0.15 \\ 0.98 & 1.41 & 1.32 & 0.59 & 0.51 & 0.2 \\ 1.01 & 1.66 & 1.57 & 0.57 & 0.56 & 0.29 \end{pmatrix}, \quad W = \begin{pmatrix} 0.8 & 0.07 & 0.1 & 0.81 \\ 0.07 & 0.51 & 0.78 & 0.4 \\ 0.77 & 0.92 & 0.4 & 0.76 \\ 0.47 & 0.9 & 0.51 & 0.7 \\ 0.58 & 0.9 & 0.87 & 0.59 \end{pmatrix}.$$

We compute H with SHAMANS with a constraint of average column-wise sparsity $k = 3$, that is, a matrix-wise constraint $q = 3 \times 6 = 18$. Table 1 shows the output of the homotopy algorithm, that is, the regularization path containing the solutions for all possible values of λ for each column.

From these paths, we can trivially get the solution to the unpenalized problem $\min_{H \geq 0} \|M - WH\|_F^2$ by selecting the last solution for each column. We can also trivially select column-wise the k -sparse solution. To select the best solution with respect to a matrix-wise sparsity constraint, SHAMANS needs extra steps. Tables 2 and 3 show respectively the corresponding matrices \mathcal{C} , and $\Delta\mathcal{C}$. Table 4 shows the corresponding matrix \mathcal{G} at different steps of the selection process.

With a 3-sparse column-wise selection, the result is H_{ks} shown in (12), for a relative reconstruction error $\frac{\|M - WH\|_F}{\|M\|_F} = 4.50\%$. With SHAMANS with $q = 18$, that is, with average 3-sparse columns is H_{Sh} shown in (12), and has a relative reconstruction error of 0.73%:

$$H_{ks} = \begin{pmatrix} 0.0 & 0.0 & 0.0 & 0.49 & 0.0 & 0.0 \\ 0.19 & 0.42 & 0.38 & 0.0 & 0.45 & 0.03 \\ 0.21 & 0.38 & 0.88 & 0.0 & 0.16 & 0.31 \\ 1.04 & 1.38 & 0.75 & 0.49 & 0.02 & 0.0 \end{pmatrix}, \quad H_{Sh} = \begin{pmatrix} 0.2 & 0.79 & 0.06 & 0.49 & 0.0 & 0.0 \\ 0.16 & 0.32 & 0.37 & 0.0 & 0.46 & 0.03 \\ 0.28 & 0.66 & 0.9 & 0.0 & 0.16 & 0.31 \\ 0.85 & 0.61 & 0.69 & 0.5 & 0.0 & 0.0 \end{pmatrix}. \quad (12)$$

Table 1 Regularization paths corresponding to $\min_{x \geq 0} \|M(:, j) - Wx\|_2^2 + \lambda \|x\|_1$, computed with the homotopy algorithm. Columns 2 to 5 are not shown.

(a) Column 1

Solutions x_t^*	$\begin{pmatrix} 0.0 \\ 0.0 \\ 0.0 \end{pmatrix}$	$\begin{pmatrix} 0.0 \\ 1.15 \\ 0.0 \end{pmatrix}$	$\begin{pmatrix} 0.0 \\ 0.34 \\ 1.05 \end{pmatrix}$	$\begin{pmatrix} 0.0 \\ 0.19 \\ 0.21 \\ 1.04 \end{pmatrix}$	$\begin{pmatrix} 0.2 \\ 0.16 \\ 0.28 \\ 0.85 \end{pmatrix}$
λ	3.16	2.75	0.25	0.06	0.0
Error $\ M(:, 1) - Wx_t^*\ _2^2$	4.31	0.67	0.02	0.0	0.0
k	0	1	2	3	4
[...]					

(b) Column 6

Solutions x_t^*	$\begin{pmatrix} 0.0 \\ 0.0 \\ 0.0 \\ 0.0 \end{pmatrix}$	$\begin{pmatrix} 0.0 \\ 0.26 \\ 0.0 \\ 0.0 \end{pmatrix}$	$\begin{pmatrix} 0.0 \\ 0.03 \\ 0.31 \\ 0.0 \end{pmatrix}$
λ	0.71	0.37	0.0
Error $\ M(:, 6) - Wx_t^*\ _2^2$	0.21	0.03	0.0
k	0	1	2

Table 2 Matrix \mathcal{C} , where every entry $\mathcal{C}(k, j)$ represents the error of the k -sparse solution of the column j , $\mathcal{C}(k, j) = \|M(:, j) - W\text{Sol}_{k,j}\|_2^2$.

k	j	1	2	3	4	5	$n = 6$
0		4.31	9.81	7.70	1.95	0.94	0.21
1		0.67	1.24	0.59	0.03	0.01	0.03
2		0.02	0.09	0.24	0.0	0.0	0.0
3		0.0	0.05	0.0	0.0	0.0	0.0
$r = 4$		0.0	0.0	0.0	0.0	0.0	0.0

Table 3 Matrix $\Delta\mathcal{C}$, where every entry $\Delta\mathcal{C}(k, j)$ represents the error decrease by going in column j from the $(k - 1)$ -sparse solution to the k -sparse one, $\Delta\mathcal{C}(k, j) = \mathcal{C}(k - 1, j) - \mathcal{C}(k, j)$.

k	j	1	2	3	4	5	$n = 6$
1		3.64	8.57	7.11	1.92	0.93	0.19
2		0.65	1.14	0.35	0.03	0.01	0.03
3		0.01	0.05	0.24	0.0	0.0	0.0
$r = 4$		0.0	0.05	0.0	0.0	0.0	0.0

4.2 Optimality and computational cost of SHAMANS

In the following two paragraphs, we discuss the optimality and the computational cost of SHAMANS.

Optimality Interestingly, although SHAMANS is a greedy algorithm as it performs an optimal selection at each iteration, it is globally optimal. The reason is that the columns of H do not interact with each other in the objective function (see Section 1.2), so the greedy solution cannot possibly be improved.

Table 4 Matrix \mathcal{G} during the first three iterations of the selection step of SHAMANS. Every entry represents the error decrease of a solution divided by its cost in sparsity budget (the number by which we need to increment the cursor of its column in order to select this solution). Every entry is initialized so that $\mathcal{G}(k, j) = (\sum_{l=1}^k \Delta\mathcal{C}(l, j))/i$. When an entry is selected, we update the other entries of this column to account for the new error decrease and cursor value. Below, the boxed entry is the maximum of the matrix, so it is the entry to be selected next.

(a) Initialization

	j	1	2	3	4	5	$n = 6$
k							
1		3.64	8.57	7.11	1.92	0.93	0.19
2		2.15	4.86	3.73	0.97	0.47	0.11
3		1.44	3.25	2.57	0.65	0.31	0.07
$r = 4$		1.08	2.45	1.93	0.49	0.24	0.05

(b) After one iteration

	j	1	2	3	4	5	$n = 6$
k							
1		3.64	0.0	7.11	1.92	0.93	0.19
2		2.15	1.14	3.73	0.97	0.47	0.11
3		1.44	0.6	2.57	0.65	0.31	0.07
$r = 4$		1.08	0.41	1.93	0.49	0.24	0.05

(c) After two iterations

	j	1	2	3	4	5	$n = 6$
k							
1		3.64	0.0	0.0	1.92	0.93	0.19
2		2.15	1.14	0.35	0.97	0.47	0.11
3		1.44	0.6	0.29	0.65	0.31	0.07
$r = 4$		1.08	0.41	0.20	0.49	0.24	0.05

Proposition 1 *The selection step of SHAMANS is guaranteed to select the best solution H with average $(q+p)/n$ -sparse columns among the set of solutions returned by the homotopy algorithm, where $p \in [0, r - 1]$, meaning that $\|H\|_0 \leq q + p$.*

Indeed, SHAMANS selects the best solution in terms of reducing the error $\|M - WH\|_F^2$ for a fixed sparsity budget, since the largest entry of \mathcal{G} is selected, while the columns of H do not interact with each other in the objective. Note that SHAMANS adds non-zero entries in H as long as $\|H\|_0 < q$, and it adds at each iteration at most r non-zero entries in a column (a column could change from the zero vector to the unconstrained NNLS solution with potentially r non-zero entries). In this particular case, the solution produced by SHAMANS could reach a sparsity of $\|H\|_0 = q + r - 1$. However, this is not an important drawback for three reasons:

- Only the last updated column can lead to the q -sparsity constraint to be violated. Moreover, since $n \gg r$, we have $(q + r)/n \approx q/n$ and this does not play an important role in practice.
- If the constraint $\|H\|_0 \leq q$ is critical, it suffices to keep the penultimate solution generated by SHAMANS.
- In most cases, we have observed that each iteration of SHAMANS only increases the number of non-zero entries in H by one; see for example Table 4. However,

there are some pathological cases where SHAMANS may increase that number by more than one.

Note that the homotopy step is approximate, so SHAMANS does not solve Problem (7) optimally in general. What SHAMANS does optimally is to select a q -sparse solution H from a set of solutions provided (in our case, by the homotopy algorithm).

Computational cost The selection step consists in building $\Delta\mathcal{C}$ in $\mathcal{O}(rn)$, building \mathcal{G} in $\mathcal{O}(rn)$, then iterating q times to select a solution. As we maintain updated a sorted list to avoid recomputing the maximum at each iteration, this is done in $\mathcal{O}(q \log(n))$. Assuming q is in the order of rn , the cost of the selection step is hence dominated by the cost of the homotopy step, that requires at least $\mathcal{O}(r^3n)$ operations to solve n NNLS problems via homotopy in r variables; see Section 3.3.

5 Experiments

In this section, we study the performance of SHAMANS on the unmixing of 7 datasets: 3 faces datasets and 4 hyperspectral images.

5.1 Data

For the faces datasets, each column of M corresponds to a pixel and each row to an image (that is, $M(i, j)$ is the intensity of pixel j in image i). It is well-known that NMF will extract facial features as the rows of matrix H (Lee and Seung, 1999). As no groundtruth is available, we first compute W with SNPA (Gillis, 2014a), an algorithm for separable NMF, setting the factorization rank r as in the literature. We then compute H with our sparsity-enhancing method. Imposing sparsity on H means that we require that only a few pixels are contained in each facial feature (Hoyer, 2004). We consider the 3 widely used face datasets CBCL³, Frey⁴, and Kuls⁵.

Similarly as for the faces, a hyperspectral image is an image-by-pixel matrix where each image corresponds to a different wavelength. The columns of W represent the spectral signature of the pure materials (also called endmembers) present in the image (Bioucas-Dias et al, 2012), and we use the ground truth W of Zhu (2017). We compute H , whose columns represent the abundance of materials in each pixel. It makes sense to impose H to be sparse as most pixels contain only a few endmembers (Ma et al, 2013). We consider the 4 widely used datasets⁶, Jasper, Samson, Urban, and Cuprite. The characteristics of the considered datasets are summarized in Table 5.

³ Downloaded from <http://poggio-lab.mit.edu/codedatasets>

⁴ Downloaded from <https://cs.nyu.edu/~roweis/data.html>

⁵ Downloaded from <http://www.robots.ox.ac.uk/>

⁶ Downloaded from <http://lesun.weebly.com/hyperspectral-data-set.html>

Table 5 Summary of the datasets studied in this work. $M \in \mathbb{R}^{m \times n}$ and $W \in \mathbb{R}^{m \times r}$.

Dataset	Type	m	n	r
CBCL	Faces	2429	$19 \times 19 = 361$	49
Frey	Faces	1965	$20 \times 28 = 560$	36
Kuls	Faces	20	$64 \times 64 = 4096$	5
Jasper	Hyperspectral	198	$100 \times 100 = 1000$	4
Samson	Hyperspectral	156	$95 \times 95 = 9025$	3
Urban	Hyperspectral	162	$307 \times 307 = 94249$	6
Cuprite	Hyperspectral	188	$250 \times 191 = 47750$	12

5.2 Methods

We compare the performances of SHAMANS with three other approaches:

- Homotopy with no sparsity constraint, noted *H no-s*. It consists in computing the homotopy path for each column and keep the best solution.
- Homotopy with a column-wise k -sparse constraint, noted *H k-s*. It consists in computing the homotopy path for each column and keep the corresponding k -sparse solution.
- NNOLS (Nguyen et al, 2019). This greedy algorithm is one of the best performing heuristic for k -sparse NNLS.

To the best of our knowledge, no other algorithm tackles the problem of MNNLS with a matrix-wise q -sparsity constraint.

We choose the parameter k by trial-and-error. Unless stated otherwise, we define the sparsity parameter of SHAMANS as $q = k \times n$, which is equivalent to an average column-wise k -sparsity constraint.

The homotopy algorithm and SHAMANS are implemented in Julia, and ran with Julia 1.5. For NNOLS, we use the Matlab implementation provided by the authors, and run it in Matlab R2019b. All experiments are made on a computer with a processor Intel Core i5-2520M @2.50GHz. The code and experiments scripts are provided in an online repository⁷.

For every dataset, we run the four methods, and measure the average sparsity of the given solutions (defined as number of entries superior to 10^{-3} divided by the number of columns), the relative reconstruction error $\frac{\|M-WH\|_F}{\|M\|_F}$, and the computing time, for which we measure the median over 10 runs. Note that, for a given dataset, a given algorithm always gives the same output.

5.3 Results and interpretation

The results of our experiments are shown in Table 6. Some abundance maps for Kuls, Jasper, and Urban are shown respectively in Figs. 3 to 5. Images from the other experiments are available as a supplementary material.

The results show that, without sparsity constraint, the resulting factors are already quite sparse. The column-wise sparse methods (H k -s and NNOLS) produce factors with an average sparsity below the sparsity threshold k , meaning that many columns actually have a sparsity level lower than the threshold. H k -s gives

⁷ <https://gitlab.com/nnadisic/giant.jl>

Table 6 Results of the experiments, for the unmixing of faces and hyperspectral datasets. Time is in seconds, relative error is in percent, and sparsity is the average number of entries above 10^{-3} . Jasper is processed once with all algorithms for $k = q/n = 2$, and once with SHAMANS for $q/n = 1.8$ (which is not possible with other algorithms).

		H no-s	H k -s	SHAMANS	NNOLS
CBCL	Time	0.78	0.77	0.84	0.26
	$r = 49$ Rel error	12.04	16.19	13.22	12.60
	$k = 3$ Sparsity	6.53	2.69	3.0	2.71
Frey	Time	1.31	1.32	1.46	0.86
	$r = 36$ Rel error	19.35	23.22	20.75	20.30
	$k = 6$ Sparsity	12.17	5.51	6.0	5.53
Kuls	Time	0.25	0.21	0.30	1.87
	$r = 5$ Rel error	19.05	20.13	19.12	19.20
	$k = 3$ Sparsity	3.44	2.86	3.0	2.84
Jasper	Time	0.63	0.63	0.74	2.25
	$r = 4$ Rel error	5.71	6.99	5.72	6.09
	$k = 2$ Sparsity	2.27	1.79	2.0	1.81
Jasper $q/n = 1.8$	Time			0.65	
	$r = 4$ Rel error			5.95	
	Sparsity			1.8	
Samson	Time	0.33	0.33	0.45	1.96
	$r = 3$ Rel error	3.3	3.34	3.30	3.34
	$k = 2$ Sparsity	2.14	1.84	2.0	1.83
Urban	Time	6.67	6.55	10.73	22.04
	$r = 6$ Rel error	7.67	8.62	7.83	8.14
	$k = 2$ Sparsity	2.61	1.90	2.0	1.90
Cuprite	Time	17.83	20.27	22.31	36.30
	$r = 12$ Rel error	1.74	2.37	2.01	2.04
	$k = 4$ Sparsity	6.60	3.93	4.0	3.93

relatively bad results in terms of error, comparing with the unconstrained solution, while SHAMANS is able to enforce sparsity while limiting the loss in error. H k -s is as fast as the unconstrained method, as expected. SHAMANS is only slightly slower, meaning that the selection step takes less time than the homotopy step, as expected in Section 4.2. These methods are faster than NNOLS for all datasets except CBCL and Frey.

NNOLS outperforms our approach in terms of error for CBCL and Frey. This means that the column-wise sparsity is a good assumption for these datasets, and also that our homotopy step does not give good enough solutions. However, SHAMANS outperforms NNOLS for all the other datasets. This verifies our assumption that columns have different sparsity levels, a situation in which our approach is especially interesting. Another advantage of the matrix-wise constraint over the column-wise one is the possibility of tuning the parameter more precisely. This is illustrated with the result for Jasper with $q/n = 1.8$ (that is, we require an average k -sparsity with $k = 1.8$), for which we reach an average sparsity similar to that of NNOLS with $k = 2$, and still get a lower error.

Visually, in Fig. 3, the unconstrained method already gives good results, but some features are not well separated. With the k -sparse selection, it fails to retrieve the features and sometimes produces noisier images. The results of NNOLS are better, but lack spatial coherence (some regions are pixelated; see for example the chin on the last image in Figure 3). SHAMANS produces better separated features, and a more consistent spatial coherence.



Fig. 3 Abundance maps of the unmixing of the Kuls facial images (that is, reshaped rows of W) with different algorithms. The extracted components correspond to different light directions.

In Fig. 4, we focus on the sixth endmember for the Urban dataset. It mainly shows pixels from rooftops. With no sparsity constraint, the image is very noisy and includes pixels composed of other materials. Visually, NNOLS gives almost no improvement, and worsen the spatial coherence (some regions are pixelated). H k -s removes too many pixels and most of the information for that endmember is lost. SHAMANS produces a better solution, with less noise, and a more distinct separation.

In Fig. 5, we focus on the second endmember for the Jasper dataset, corresponding to water. Without sparsity constraint, they are mixed with pixels of the road on the right. NNOLS with $k = 2$ and SHAMANS with $k = q/n = 2$ fail to separate these pixels. SHAMANS with $k = q/n = 1.8$ performs an almost perfect separation, and eliminates the non-water pixels while sharpening the edge between water and non-water pixels. In these images, it is clear that some pixels are com-

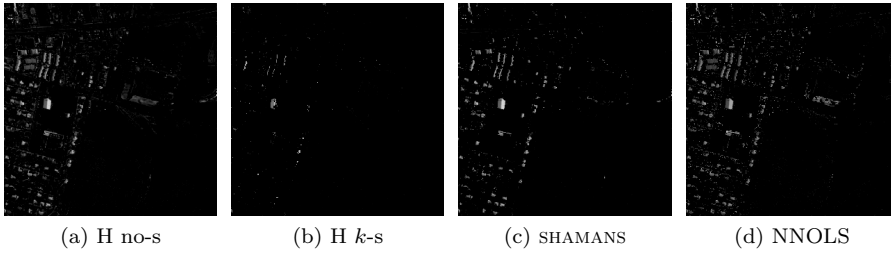


Fig. 4 Abundance maps of the sixth endmember (that is, the sixth row of H reshaped) from the unmixing of the hyperspectral image Urban by different algorithms.

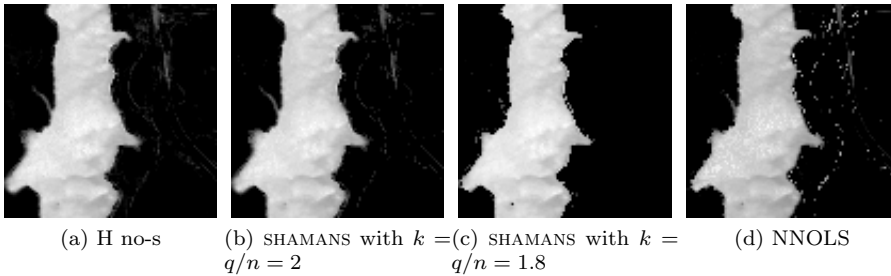


Fig. 5 Abundance maps of the second endmember (that is, the second row of H reshaped) from the unmixing of the hyperspectral image Jasper by different algorithms.

posed of only one endmember (for instance, water) while others are mixed (trees and grass mixed). This is the kind of setting where SHAMANS can bring significant improvement.

6 Conclusion

In this paper, we have focused on the sparse multiple right-hand sides NNLS problem with a matrix-wise ℓ_0 -constraint. We introduced SHAMANS (Algorithm 2), a two-step algorithm to tackle this problem, that first computes for each column the regularization path of the ℓ_1 -penalized subproblem via a homotopy algorithm, and then applies a selection strategy to build the solution matrix H from these paths. Our method solves exactly the selection subproblem. We illustrated the advantages of SHAMANS for the unmixing of facial and hyperspectral images, for which it generally outperformed the state-of-the-art heuristic NNOLS in both reconstruction error and computing time. SHAMANS is particularly useful for datasets for which the columns of H have different sparsity levels. Also, it is almost as fast as a standard active-set algorithms for NNLS with no sparsity constraint, and thus can be applied to large datasets.

Acknowledgements We thank Maxime De Wolf for his technical contribution to the implementation of our methods. We thank T.T. Nguyen and his co-authors for making the codes of nonnegative greedy algorithms available online under a free software license.

References

- Aharon M, Elad M, Bruckstein AM (2005) K-SVD and its non-negative variant for dictionary design. In: Wavelets XI, International Society for Optics and Photonics
- Bertsimas D, Shioda R (2009) Algorithm for cardinality-constrained quadratic optimization. *Computational Optimization and Applications* 43(1):1–22
- Bienstock D (1996) Computational study of a family of mixed-integer quadratic programming problems. *Mathematical programming* 74(2):121–140
- Bioucas-Dias JM, Plaza A, Dobigeon N, Parente M, Du Q, Gader P, Chanussot J (2012) Hyperspectral unmixing overview: Geometrical, statistical, and sparse regression-based approaches. *IEEE Journal of Selected Topics in Applied Earth Observations and Remote Sensing* 5(2):354–379
- Bourguignon S, Ninin J, Carfantan H, Mongeau M (2015) Exact sparse approximation problems via mixed-integer programming: Formulations and computational performance. *IEEE Transactions on Signal Processing* 64(6):1405–1419
- Chen S, Billings SA, Luo W (1989) Orthogonal least squares methods and their application to non-linear system identification. *International Journal of control* 50(5):1873–1896
- Cichocki A, Phan AH, Caiafa C (2008) Flexible HALS algorithms for sparse non-negative matrix/tensor factorization. In: *IEEE Workshop on Machine Learning for Signal Processing*, pp 73–78
- Cohen JE, Gillis N (2019) Nonnegative Low-rank Sparse Component Analysis. In: *2019 IEEE International Conference on Acoustics, Speech and Signal Processing*, pp 8226–8230
- Donoho DL, Tsaig Y (2008) Fast Solution of ℓ_1 -Norm Minimization Problems When the Solution May Be Sparse. *IEEE Trans Inform Theory* 54(11):4789–4812
- Efron B, Hastie T, Johnstone I, Tibshirani R, et al (2004) Least angle regression. *The Annals of statistics* 32(2):407–499
- Eggert J, Korner E (2004) Sparse coding and NMF. In: *IEEE International Joint Conference on Neural Networks*, vol 4, pp 2529–2533
- Foucart S, Koslicki D (2014) Sparse recovery by means of nonnegative least squares. *IEEE Signal Processing Letters* 21(4):498–502
- Gillis N (2012) Sparse and unique nonnegative matrix factorization through data preprocessing. *Journal of Machine Learning Research* 13:3349–3386
- Gillis N (2014a) Successive Nonnegative Projection Algorithm for Robust Nonnegative Blind Source Separation. *SIAM Journal on Imaging Sciences* 7(2):1420–1450
- Gillis N (2014b) The why and how of nonnegative matrix factorization. *Regularization, Optimization, Kernels, and Support Vector Machines* 12(257):257–291
- Hoyer PO (2002) Non-negative sparse coding. In: *IEEE Workshop On Neural Networks for Signal Processing*, pp 557–565
- Hoyer PO (2004) Non-negative matrix factorization with sparseness constraints. *Journal of machine learning research* 5:1457–1469
- Itoh Y, Duarte MF, Parente M (2017) Perfect Recovery Conditions For Non-Negative Sparse Modeling. *IEEE Transactions on Signal Processing* 65(1):69–80
- Kim H, Park H (2007) Sparse non-negative matrix factorizations via alternating non-negativity-constrained least squares for microarray data analysis. *Bioinform-*

- atics 23(12):1495–1502
- Kim J, Ramakrishnan N, Marwah M, Shah A, Park H (2013) Regularization Paths for Sparse Nonnegative Least Squares Problems with Applications to Life Cycle Assessment Tree Discovery. In: IEEE 13th International Conference on Data Mining, pp 360–369
- Lawson CL, Hanson RJ (1995) Solving least squares problems. Society for Industrial and Applied Mathematics
- Lee DD, Seung HS (1997) Unsupervised learning by convex and conic coding. In: Advances in neural information processing systems, pp 515–521
- Lee DD, Seung HS (1999) Learning the parts of objects by non-negative matrix factorization. *Nature* 401(6755):788–791
- Ma WK, Bioucas-Dias JM, Chan TH, Gillis N, Gader P, Plaza AJ, Ambikapathi A, Chi CY (2013) A signal processing perspective on hyperspectral unmixing: Insights from remote sensing. *IEEE Signal Processing Magazine* 31(1):67–81
- Mhenni R, Bourguignon S, Ninin J (2019) Global optimization for sparse solution of least squares problems. <https://hal.archives-ouvertes.fr/hal-02066368/>
- Morup M, Madsen KH, Hansen LK (2008) Approximate L0 constrained non-negative matrix and tensor factorization. In: 2008 IEEE International Symposium on Circuits and Systems, IEEE, pp 1328–1331
- Nadisic N, Vandaele A, Gillis N, Cohen JE (2020) Exact Sparse Nonnegative Least Squares. In: ICASSP 2020, pp 5395 – 5399
- Nguyen TT, Idier J, Soussen C, Djermoune EH (2019) Non-Negative Orthogonal Greedy Algorithms. *IEEE Transactions on Signal Processing* pp 1–16
- Osborne MR, Presnell B, Turlach BA (2000) A new approach to variable selection in least squares problems. *IMA journal of numerical analysis* 20(3):389–403
- Pati YC, Rezaifar R, Krishnaprasad PS (1993) Orthogonal matching pursuit: Recursive function approximation with applications to wavelet decomposition. In: Proceedings of 27th Asilomar Conference on Signals, Systems and Computers, pp 40–44
- Peharz R, Pernkopf F (2012) Sparse nonnegative matrix factorization with l0-constraints. *Neurocomputing* 80:38–46
- Soussen C, Gribonval R, Idier J, Herzet C (2013) Joint k -Step Analysis of Orthogonal Matching Pursuit and Orthogonal Least Squares. *IEEE Transactions on Information Theory* 59(5):3158–3174
- Tibshirani R (1996) Regression shrinkage and selection via the lasso. *Journal of the Royal Statistical Society: Series B (Methodological)* 58(1):267–288
- Tropp JA (2006) Just relax: convex programming methods for identifying sparse signals in noise. *IEEE Transactions on Information Theory* 52(3):1030–1051
- Zhu F (2017) Hyperspectral unmixing: ground truth labeling, datasets, benchmark performances and survey. arXiv preprint arXiv:170805125

Supplementary material for the paper “A Homotopy-based Algorithm for Sparse Multiple Right-hand Sides Nonnegative Least Squares”

In this document, we provide the abundance maps resulting from our experiments, that could not be included in the paper:

- CBCL in Figure 6,
- Frey in Figure 7,
- Jasper in Figure 8,
- Samson in Figure 9,
- Urban in Figure 10, and
- Cuprite in Figure 11.

As explained in the paper, the abundance maps generated by SHAMANS tends to be less noisy and less pixelated compare to the other sparse MNNLS algorithms.

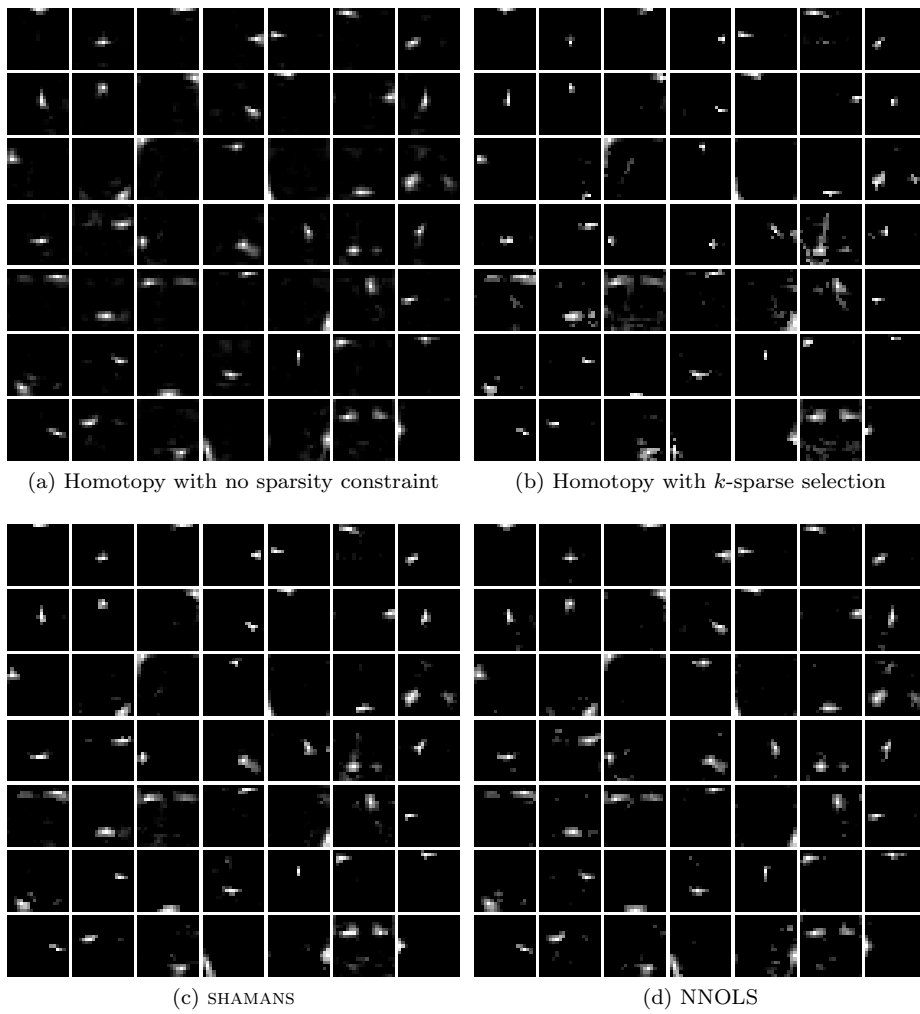


Fig. 6 Abundance maps of the unmixing of the CBCL facial images (that is, reshaped rows of W) with different algorithms.

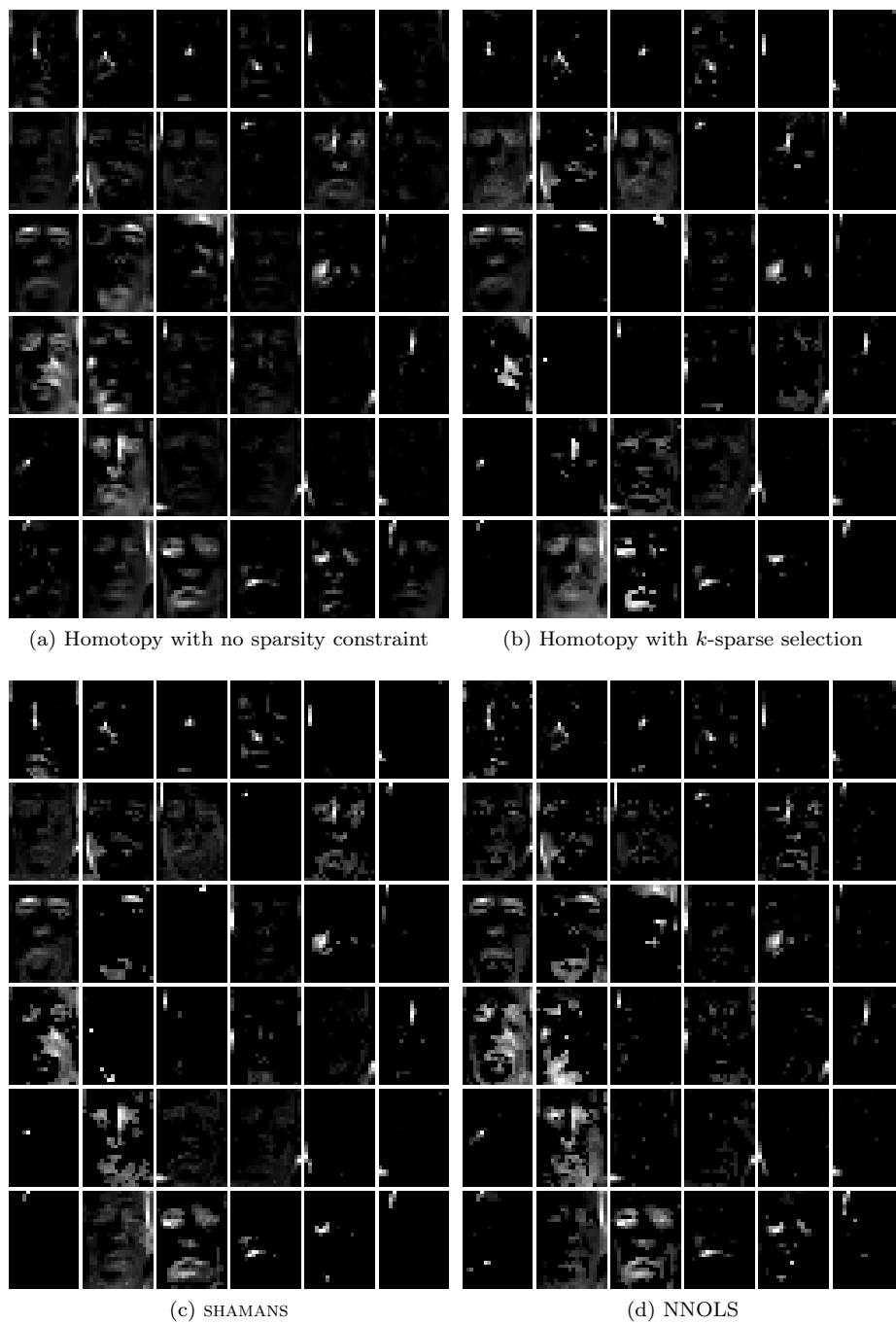
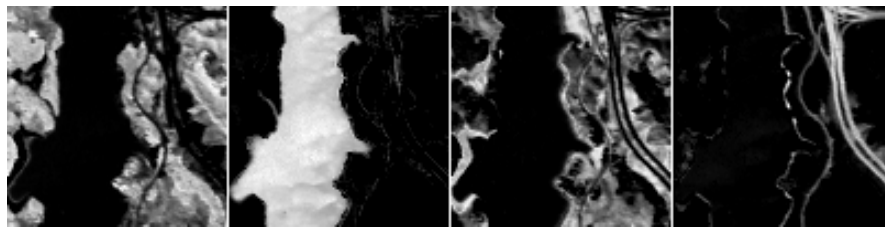
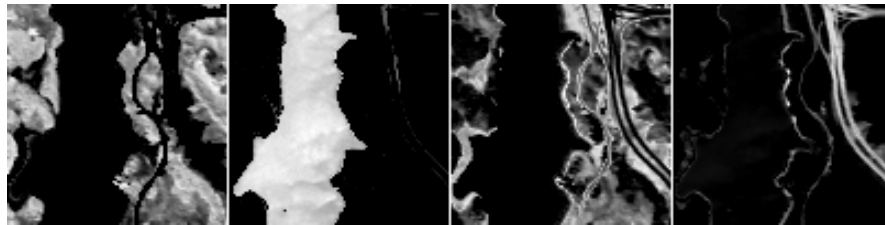
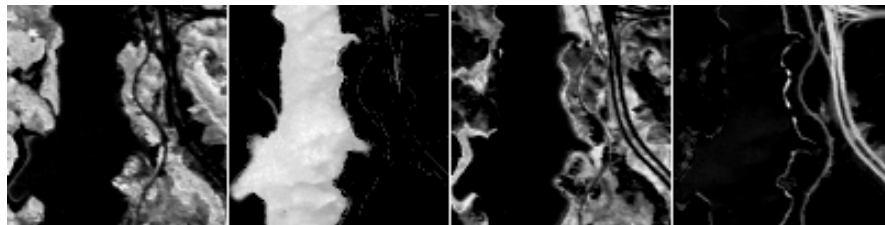
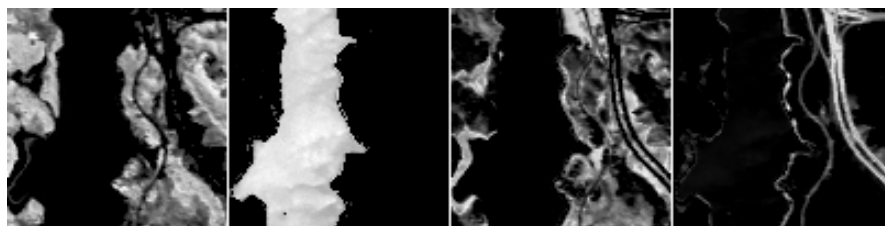
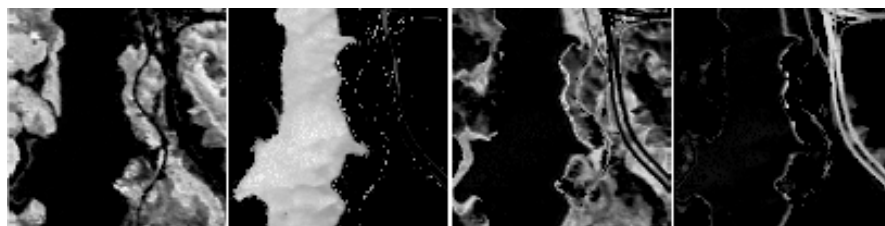


Fig. 7 Abundance maps of the unmixing of the Frey facial images (that is, reshaped rows of W) with different algorithms.

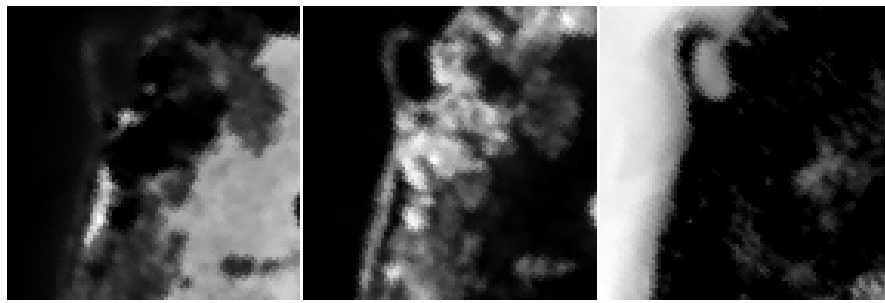


(a) Homotopy with no sparsity constraint

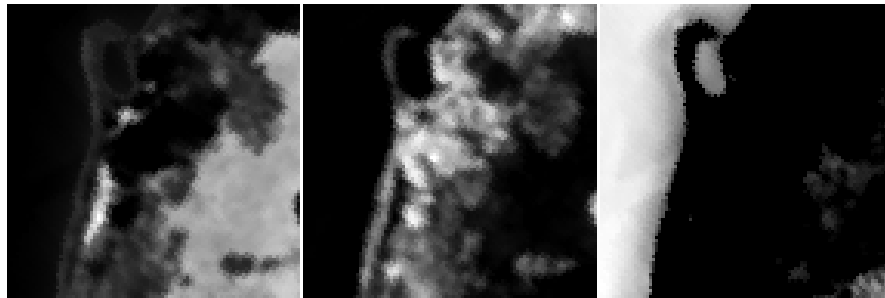
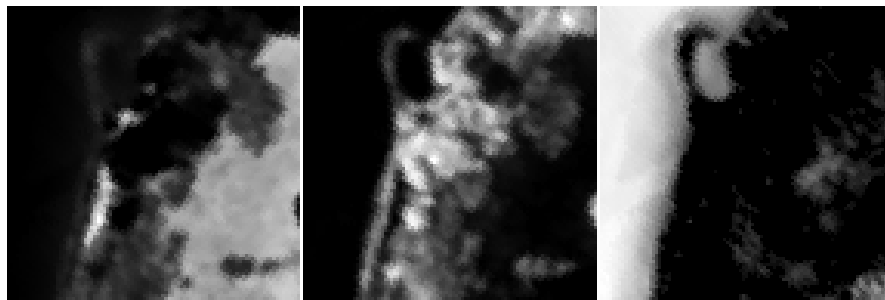
(b) Homotopy with k -sparse selection(c) SHAMANS with $q = 20000$ (d) SHAMANS with $q = 18000$ 

(e) NNOLS

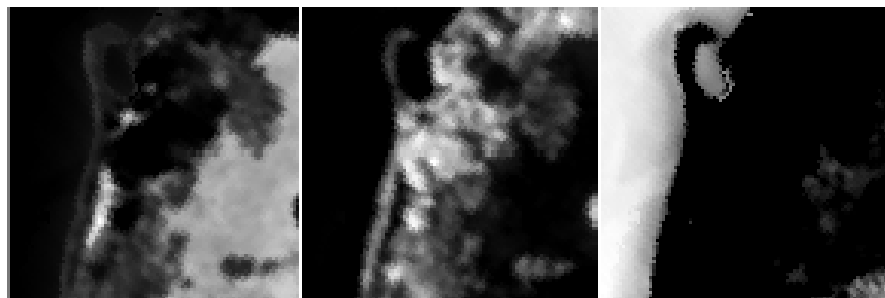
Fig. 8 Abundance maps (that is, reshaped rows of H) from the unmixing of the hyperspectral image Jasper by different algorithms.



(a) Homotopy with no sparsity constraint

(b) Homotopy with k -sparse selection

(c) SHAMANS



(d) NNOLS

Fig. 9 Abundance maps (that is, reshaped rows of H) from the unmixing of the hyperspectral image Samson by different algorithms.



(a) Homotopy with no sparsity constraint

(b) Homotopy with k -sparse selection

(c) SHAMANS



(d) NNOLS

Fig. 10 Abundance maps (that is, reshaped rows of H) from the unmixing of the hyperspectral image Urban by different algorithms.

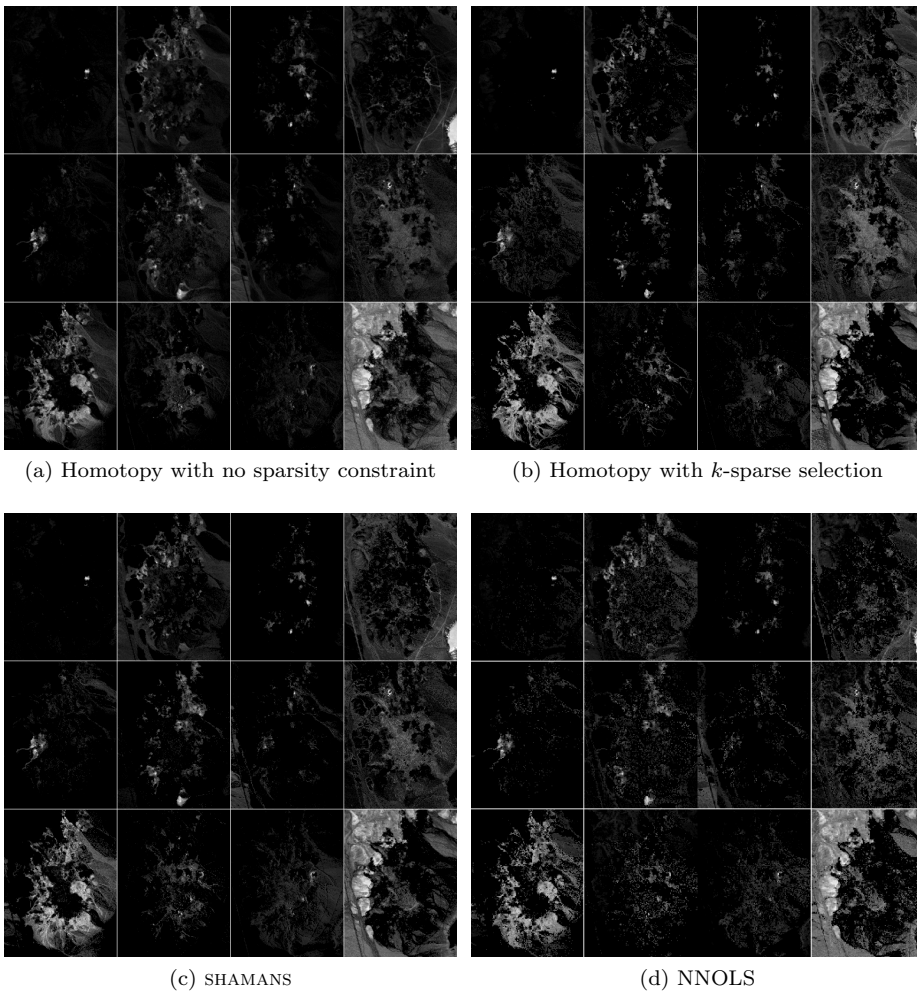


Fig. 11 Abundance maps (that is, reshaped rows of H) from the unmixing of the hyperspectral image Cuprite by different algorithms.